

**DESIGN AND PERFORMANCE EVALUATION OF AN
INTEGRATED SOLAR DRYER FOR FISH AND
MARINE PRODUCTS THROUGH COMPUTATIONAL
FLUID DYNAMICS SIMULATION**



ADELINE TAN SHU TING

UMS
UNIVERSITI MALAYSIA SABAH

**FACULTY OF ENGINEERING
UNIVERSITI MALAYSIA SABAH
2023**

**DESIGN AND PERFORMANCE EVALUATION OF AN
INTEGRATED SOLAR DRYER FOR FISH AND
MARINE PRODUCTS THROUGH COMPUTATIONAL
FLUID DYNAMICS SIMULATION**

ADELINE TAN SHU TING



UMS

**THESIS SUBMITTED IN FULFILLMENT OF THE
REQUIREMENTS FOR THE DEGREE OF
MASTER OF ENGINEERING**

**FACULTY OF ENGINEERING
UNIVERSITI MALAYSIA SABAH
2023**

UNIVERSITI MALAYSIA SABAH
BORANG PENGESAHAN STATUS TESIS

JUDUL : **DESIGN AND PERFORMANCE EVALUATION OF AN INTEGRATED SOLAR DRYER FOR FISH AND MARINE PRODUCTS THROUGH COMPUTATIONAL FLUID DYNAMICS SIMULATION**

IJAZAH : **SARJANA KEJURUTERAAN**

BIDANG : **KEJURUTERAAN KIMIA**

Saya **ADELINE TAN SHU TING**, Sesi **2020-2023**, mengaku membenarkan tesis Sarjana ini disimpan di Perpustakaan Universiti Malaysia Sabah dengan syarat-syarat kegunaan seperti berikut:-

1. Tesis ini adalah hak milik Universiti Malaysia Sabah
2. Perpustakaan Universiti Malaysia Sabah dibenarkan membuat salinan untuk tujuan pengajian sahaja.
3. Perpustakaan dibenarkan membuat salinan tesis ini sebagai bahan pertukaran antara institusi pengajian tinggi.

4. Sila tandakan (/):

SULIT

(Mengandungi maklumat yang berdarjah keselamatan atau kepentingan Malaysia seperti yang termaktub di dalam AKTA RAHSIA 1972)

TERHAD


(Mengandungi maklumat TERHAD yang telah ditentukan oleh organisasi/badan di mana penyelidikan dijalankan)

/ TIDAK TERHAD

Disahkan Oleh,



ADELINE TAN SHU TING
MK2011011T

 ANITA BINTI ARSAD
PUSTAKAWAN KANAN
UNIVERSITI MALAYSIA SABAH

(Tandatangan Pustakawan)


Tarikh : 21 February 2023

(Assoc. Prof. Dr. Jidon @ Adrian Bin Janaun)
Penyelia Utama

DECLARATION

I hereby declare that the material in this thesis is my own except for quotations, equations, summaries, and references, which have been duly acknowledged.

12 April 2023



Adeline Tan Shu Ting

MK2011011T



UMMS
UNIVERSITI MALAYSIA SABAH

CERTIFICATION

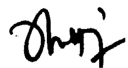
NAME : **ADELINE TAN SHU TING**
MATRIC NO. : **MK2011011T**
TITLE : **DESIGN AND PERFORMANCE EVALUATION OF AN INTEGRATED SOLAR DRYER FOR FISH AND MARINE PRODUCTS THROUGH COMPUTATIONAL FLUID DYNAMICS SIMULATION**
DEGREE : **MASTER OF ENGINEERING**
FIELD : **CHEMICAL ENGINEERING**
VIVA DATE : **12 APRIL 2023**



CERTIFIED BY;
UMS
UNIVERSITI MALAYSIA SABAH
Signature

- 1. MAIN SUPERVISOR**
Assoc. Prof. Dr. Jidon @ Adrian Bin
Janaun
- 2. CO-SUPERVISOR**
Assoc. Prof. Ts. Dr. Nancy Julius Siambun
- 3. CO-SUPERVISOR**
Dr. Tham Heng Jin





ACKNOWLEDGEMENTS

I would like to acknowledge and give my warmest thanks to my supervisor Assoc. Prof. Dr. Jidon @ Adrian Bin Janaun who made this work possible. His guidance and advice carried me through all the stages of conducting this research. I would also like to thank my co-supervisors Assoc. Prof. Ts. Dr. Nancy Julius Siambun and Dr. Tham Heng Jin providing me valuable suggestion when undertaking my research and writing my project. I would also like to acknowledge Dr. Ng Chi Huey who provided positive feedback and brilliant comments and suggestions on my work.

In addition, I would like to express my gratitude to all my friends and family members who have stood by my side, giving me continuous support and understanding throughout this journey.

Finally, I gratefully acknowledge the funding and scholarship received towards my study. First and foremost, I would like to acknowledge the Ministry of Finance Malaysia (MoF) Social Enterprise Project (Project code: R/MOF/B0108/01759A/001/2020/0072), in collaboration between Universiti Malaysia Sabah and Universiti Malaysia Kelantan (UMS Project Code: LPK2001) for supporting this study. Also, I would like to express my gratitude to Universiti Malaysia Sabah for the award of *Skim Bantuan Pascasiswazah* (SBP) scholarship for this degree.

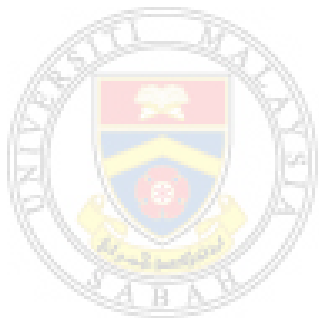
Adeline Tan Shu Ting

12 April 2023

ABSTRACT

There are several drawbacks remain to be resolved for the application of solar dryer in fish drying, such include low solar intensity, uniformity of heat distribution, and inadequate air circulation. In this present study, a mixed mode type solar dryer namely, Integrated Solar Dryer (INSOLER) was presented and the performance under pseudo natural convection was studied through Computational Fluid Dynamics (CFD) simulation under inlet mass flow rate of 0.012 kg/s and solar irradiance of 438.58 W/m². In this solar dryer, enhancement was proposed on the design of solar heat collector, air distribution system, and chimney, which governs the temperature, uniformity, and air circulation, respectively, to address the limitation mentioned. The main purpose of this research is to address the gaps in the design of these components and identify the improvements in term of heat transfer and fluid flow characteristics. The first objective of this work aimed to determine the performance of baffle-type solar heat collector (B-SHC) with different baffle arrangement, namely longitudinal SHC (L-SHC) and transversal SHC (T-SHC). It was found that L-SHC offers higher outlet temperature, collector efficiency, and thermo-hydraulic performance factor (THPF) of 59.43 °C, 46.2% and 2.1, respectively, indicating flow resistant presence in the air passage of longitudinal arrangement does not outweigh the enhancement of heat transfer in the collector. To ensure uniform heat distribution across the drying house, air distribution system with different perforation direction – upward and downward, was proposed. The latter configuration was proposed to address potential faulty operation caused by moisture accumulation and to ensure maximum heat transfer enhancement in the solar dryer. As expected, this perforation demonstrated more uniform temperature profile with p-value greater than 0.01 across different tray level and exhibits superior performance with heat transfer enhancement factor of 1.09. Followed by, three different chimney placement – exterior chimney, interior chimney, and interior chimney with perforation, were evaluated in term of the temperature distribution and the velocity profile attained across the drying house. Interior chimney was proposed to prevent continuous outflow of air which ultimately promotes heat accumulation in the dryer. Interior

chimney with perforation demonstrated highest temperature with a value of 67 °C and the velocity profile obtained implied extended air residence time in the solar dryer due to the presence of greater air resistance. Lastly, INSOLER developed with the combination of these improvements offers drying temperature range suitable for the drying of fish (maximum temperature = 66 °C), uniform temperature profile across different tray level (p-value>0.01), and air circulation that promote heat accumulation in the drying area, which compensated the limitations of solar dryer mentioned earlier. For optimization purpose, the performance of INSOLER under different mass flow rate and solar irradiance was also studied. It was revealed that there is a difficulty in compromising between attaining allowable temperature range and better uniformity. With these findings obtained, this research could serve as a baseline study for the implementation of solar heat collector, air distribution, and chimney design covered in this work as a continuous effort for solar dryer enhancement to achieve sustainable development in food processing industry.



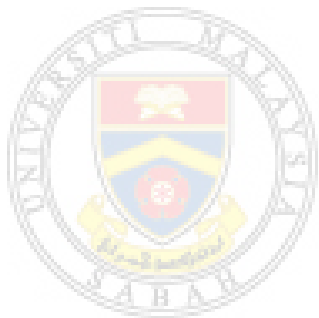
UMS
UNIVERSITI MALAYSIA SABAH

ABSTRAK

REKA BENTUK DAN PENILAIAN PRESTASI PENGERING SOLAR UNTUK PRODUK-PRODUK IKAN DAN LAUTAN MELALUIS SIMULASI COMPUTATIONAL FLUID DYNAMICS

Terdapat beberapa kelemahan yang masih perlu diatasi bagi menggunakan sistem pengering suria untuk pengeringan bahan makanan seperti tenaga haba yang tidak mencukupi, pengagihan haba yang tidak homogen, dan peredaran udara yang kurang memuaskan. Dalam kajian ini, pengering suria jenis 'mixed-mode' dinamakan Integrated Solar Dryer (INSOLER) telah direka bentuk dan seterusnya diuji di bawah pseudo natural convection (aliran jisim 0.012 kg/s, solar sinaran 438.58W/m²) menggunakan simulasi Computational Fluid Dynamics (CFD). Oleh itu, kajian ini memberi fokus kepada manambah baik kecekapan sistem pengering suria dari segi rekaan pengumpul suria (SHC), sistem peredaran haba dan cerobong. Dalam kajian ini, SHC jenis baffle direka dengan konfigurasi aliran yang berbeza – longitudinal SHC (L-SHC) dan transversal SHC (T-SHC), telah dicadangkan. Prestasi terma SHC telah diramalkan dari segi ciri-ciri pemindahan haba dan aliran udara dalam pengumpul tersebut melalui simulasi CFD. Didapati bahawa L-SHC mempunyai suhu, kecekapan pengumpul dan thermo-hydraulic performance factor (THPF) yang lebih tinggi, iaitu 59.43°C, 46.20% dan 2.1. Ini menunjukkan kalis aliran dalam pengumpul tidak melebihi peningkatan pemindahan haba yang tercapai. Bagi memastikan penyebaran haba yang seragam, sistem pengedaran udara yang berlubang (perforation) telah dicadangkan. Komponen ini telah menunjukkan profil suhu yang seragam dan menunjukkan p-value lebih daripada 0.01 dan faktor peningkatan pemindahan haba sebanyak 1.09. Cerobong dengan reka bentuk yang berbeza – cerobong external, cerobong interior, dan cerobong interior berlubang, telah dinalai dari segi profil suhu dan profil aliran udara merentasi sistem ini. Didapati bahawa cerobong interior berlubang menunjukkan suhu tertinggi (67 °C) dan mempamerkan faedah tambahan bawah keadaan with-load. Akhir sekali, INSOLER dibangunkan dengan gabungan penambahbaikan ini menawarkan julat suhu pengeringan yang sesuai untuk pengeringan ikan (suhu maksimum = 66°C), profil suhu seragam (p-value>0.01), dan peredaran udara yang menggalakkan pengumpulan haba di kawasan pengeringan. Untuk tujuan pengoptimuman, prestasi INSOLER di bawah kadar aliran

jisim dan sinaran suria yang berbeza turut dikaji. Telah diramalkan bahawa terdapat kesukaran untuk berkompromi antara mencapai suhu yang dibenarkan untuk pengeringan ikan dan keseragaman yang lebih baik. Dengan penemuan ini yang diperolehi, penyelidikan ini boleh menjadi kajian asas untuk pelaksanaan pengumpul haba suria, pengagihan udara dan reka bentuk cerobong yang dikaji dalam kerja ini sebagai usaha untuk peningkatan pengering suria untuk mencapai pembangunan dalam industri pemprosesan makanan. Kesimpulannya, kesukaran untuk berkompromi antara mencapai julat suhu yang dibenarkan dan keseragaman yang lebih baik boleh diatasi dengan mengawal selia kadar aliran jisim di salur masuk pengering suria mengikut variasi sinaran suria sepanjang hari.



UMS
UNIVERSITI MALAYSIA SABAH

LIST OF CONTENTS

	Page
TITLE	i
DECLARATION	ii
CERTIFICATION	iii
ACKNOWLEDGEMENTS	iv
ABSTRACT	v
<i>ABSTRAK</i>	vii
LIST OF CONTENTS	ix
LIST OF TABLES	xiii
LIST OF FIGURES	xvi
LIST OF NOMENCLATURES	xxi
LIST OF ABBREVIATIONS	xxiv
LIST OF APPENDICES	xxv
CHAPTER 1: INTRODUCTION	
1.1 Research Background	1
1.2 Problem Statement	4
1.3 Research Questions	5
1.4 Research Objectives	6
1.5 Scope of Research	7
1.6 Significance of Research	8
1.7 Thesis Structure	8

CHAPTER 2: LITERATURE REVIEW

2.1	Drying Mechanism of Fish	9
2.1.1	Drying Techniques	10
2.1.2	Factors Affecting Fish Drying	12
2.1.3	Quality Changes in Fish and Marine Products Drying	15
2.2	Desired Quality Attributes for Dried Fish and Marine Products	17
2.2.1	Proximate Composition	17
2.2.2	Microbial Contamination	19
2.2.3	Biochemical Reaction	20
2.2.4	Sensory Evaluation	20
2.3	Optimum Drying Temperature for Fish and Marine Products Drying	24
2.3.1	Drying Characteristics of Fish and Marine Products	25
2.3.2	Water Binding Mechanism	26
2.3.3	Drying Kinetics	28
2.3.4	Effective coefficient of diffusion	29
2.4	Summary of Previous Studies on Fish Drying under Various Drying Methods	32
2.5	Conventional Drying Method	40
2.5.1	Electrical Method	40
2.5.2	Mechanical Method	40
2.5.3	Sun Drying	41
2.5.4	Solar Drying	42
2.6	Classification of Solar Dryer	43
2.6.1	Mode of Air Movement	43
2.6.2	Mode of Heat Transfer	45
2.6.3	Comparison of Different Classification Solar Dryer	47
2.6.4	Hybrid Mode	48
2.7	Design Considerations for Solar Fish Dryer	53
2.7.1	Drying Properties of Fish	53
2.7.2	Limitations of Solar Dryer for Fish Drying	55
2.8	Observations from Literature Review	75

CHAPTER 3: METHODOLOGY

3.1	Research Approach	77
3.2	Design Concept	81
3.2.1	Solar heat collector	81
3.2.2	Drying house	81
3.2.3	Chimney	82
3.3	Design Algorithm of Solar Dryer	82
3.3.1	Design Equation	83
3.4	Description of Integrated Solar Dryer	90
3.4.1	Solar heat collector	92
3.4.2	Drying house	93
3.4.3	Chimney	94
3.5	Computational Model	95
3.5.1	Solar Heat Collector	96
3.5.2	Perforated Air Distributor	102
3.5.3	Chimney	110
3.6	Experimental Validation	116
3.7	Mathematical Modelling	118
3.7.1	Modelling of Perforated Air Distributor	118
3.7.2	Modelling of Chimney	119
3.7.3	Energy Balance	120
3.8	Performance Evaluation of Solar Drying System	123
3.8.1	Solar Heat Collector	123
3.8.2	Perforated Air Distributor	124

CHAPTER 4: RESULTS AND DISCUSSION

4.1	Performance Analysis of a Baffle-type Solar Heat Collector	126
4.1.1	Temperature Distribution and Thermal Efficiency	126
4.1.2	Heat Transfer Coefficient and Nusselt Number	129
4.1.3	Fluid Flow Characteristics	131
4.1.4	Thermo-hydraulic Performance	134
4.1.5	Results of Solar Heat Collector Scale-Up model for INSOLER	135

4.2	Performance Analysis of Solar Dryer with Perforated Air Distributor	138
4.2.1	Comparison of CFD Results and Mathematical Correlation	139
4.2.2	Effect on Airflow Distribution	140
4.2.3	Effect on Temperature Distribution	145
4.2.4	Heat Transfer Enhancement	152
4.3	Performance Analysis of Solar Dryer with Different Chimney Placement	154
4.3.1	Comparison of CFD Results and Mathematical Correlation	155
4.3.2	Effect on Airflow Distribution	156
4.3.3	Effect on Temperature Distribution	160
4.4	Performance Analysis of Integrated Solar Dryer	168
4.4.1	Mesh Independence and Turbulence Model Analysis	170
4.4.2	Boundary Conditions and Solver Setup	171
4.4.3	Experimental Validation	172
4.4.4	Effect of Different Chimney Placement on Airflow Distribution in INSOLER	176
4.4.5	Effect of Different Chimney Placement on Temperature Distribution in INSOLER	180
4.5	Influence of Operating Conditions on the Performance of INSOLER	188
4.5.1	Effect of mass flow rate	189
4.5.2	Effect of solar irradiance	191
4.6	Comparative Study	193
	CHAPTER 5: CONCLUSION AND RECOMMENDATIONS	195
	REFERENCES	199
	APPENDICES	224

LIST OF TABLES

	Page
Table 2.1 : Experimental initial moisture content of different marine species (without any pre-treatment).	13
Table 2.2 : Maximum allowable moisture and salt content for dried salted seafood according to Bureau of Indian Standards.	18
Table 2.3 : Minimum water activity and the corresponding microbial growth presence.	19
Table 2.4 : Microbial activity indicators and its corresponding allowable limit for dried fish products.	20
Table 2.5 : Acceptable limit of biochemical reaction presence in dried fish products.	20
Table 2.6 : Sensory characteristics preference of dried marine products according to various species and region investigated.	22
Table 2.7 : Optimum drying condition for fish and marine products recommended in literature.	25
Table 2.8 : Equilibrium moisture content attained at water activity = 0.6 for various marine species.	27
Table 2.9 : Estimated drying time and coefficient of diffusion from drying kinetics model developed in the literature.	31
Table 2.10 : Drying condition and quality attributes of dried marine products under natural drying method.	33
Table 2.11 : Drying condition and quality attributes of dried marine products under artificial drying method.	38
Table 2.12 : Design matrix of solar dryer.	43
Table 2.13 : Summary of the advantages and disadvantages of using solar dryer with different heat transfer mode for fish and marine products drying.	48
Table 2.14 : Summary of different type solar dryer tested for fish and marine products drying.	50

Table 2.15	: A summary of solar heat collector design parameters and the corresponding enhancement mechanism reported for the application of solar dryer.	60
Table 2.16	: A summary of design features reported to enhance uniformity of air distribution in solar dryer.	70
Table 3.1	: Meteorological condition in UMS used for the sizing of INSOLER prototype.	83
Table 3.2	: Drying parameters and assumptions used for the design of solar heat collector.	83
Table 3.3	: Calculated data for the design parameter estimation of solar heat collector.	86
Table 3.4	: Drying parameters and assumptions used for the design of perforated air distributor in drying house.	87
Table 3.5	: Drying parameters and assumptions used for the design of chimney.	89
Table 3.6	: Calculated data for the design parameter estimation of chimney.	90
Table 3.7	: Grid independence test results for Longitudinal Solar Heat Collector (L-SHC).	100
Table 3.8	: Grid independence test results for Transversal Solar Heat Collector (T-SHC).	100
Table 3.9	: Material properties defined on the computational domain.	101
Table 3.10	: Boundary conditions subjected to solar heat collector with inlet velocity = 0.6 m/s.	101
Table 3.11	: Boundary conditions subjected to solar dryer with perforated air distributor with inlet velocity = 0.6 m/s.	108
Table 3.12	: Material properties defined on the computational domains.	108
Table 3.13	: Grid independence test results for case 3.	114
Table 3.14	: Boundary conditions subjected to solar dryer with chimney with inlet velocity = 0.6 m/s.	115
Table 3.15	: Calculation results of collector efficiency for multiple-pass solar heat collector (M-SHC) by CFD simulation and experimental analysis.	118

Table 4.1	: Efficiency of solar heat collector incorporated with flow modification enhancement reported in the literature and a comparison with present work.	136
Table 4.2	: P-value of drying air temperature variation obtained across the coordinate position of drying trays in the solar dryer.	150
Table 4.3	: Uniformity coefficient of drying air temperature over the surface of drying tray.	151
Table 4.4	: Parameters for heat transfer and fluid flow characteristics.	154
Table 4.5	: P-value of drying air temperature variation obtained across the coordinate position of drying trays in the solar dryer.	165
Table 4.6	: Uniformity coefficient of drying air temperature over the surface of drying tray.	166
Table 4.7	: Grid independence test for INSOLER.	170
Table 4.8	: Boundary conditions subjected to INSOLER with inlet velocity = 0.6 m/s.	172
Table 4.9	: Specifications of measuring device used for experimental validation.	174
Table 4.10	: P-value of drying air temperature variation obtained across the coordinate position of drying trays in the solar dryer.	185
Table 4.11	: Uniformity coefficient of drying air temperature over the surface of drying tray.	186
Table 4.12	: Comparison of current study with previous studies that apply CFD modelling in the analysis and performance evaluation of mixed mode and greenhouse type solar dryer for food drying.	194

LIST OF FIGURES

	Page
Figure 2.1 : Mass transfer and heat transfer processes involve in a drying process.	10
Figure 2.2 : Desorption isotherm of anchovy fish at drying temperature of 50 to 70 °C.	26
Figure 2.3 : Drying curve of anchovy dried at temperature of 50°C and airflow rate of 2.5m/s.	28
Figure 3.1 : Methodology flow-diagram	80
Figure 3.2 : A simplified psychrometric chart demonstrating the variation of	85
Figure 3.3 : Preliminary design of Integrated Solar Dryer (INSOLER).	91
Figure 3.4 : Design modification proposed for solar dryer improvement.	91
Figure 3.5 : Preliminary design of solar heat collector.	92
Figure 3.6 : Baffle-type solar heat collector with (a) Longitudinal baffle arrangement (L-SHC) and (b) Transversal baffle arrangement (T-SHC).	93
Figure 3.7 : Preliminary design of drying house installed with perforated air distributor.	94
Figure 3.8 : Preliminary design of chimney.	95
Figure 3.9 : Three-dimensional computational geometry of the solar heat collector – (a) Longitudinal Solar Heat Collector (L-SHC) and (b) Transversal Solar Heat Collector (T-SHC).	98
Figure 3.10 : Computational model of solar dryer with perforated air distributor studied – (a) Case 1: Reference case, (b) Case 2: Perforated air distributor with upward perforation, (c) Case 3: Perforated air distributor with downward perforation.	103
Figure 3.11 : (a) Pictorial view of Integrated Solar Dryer (INSOLER). (b) Computational model of INSOLER (one compartment) with dimension.	104
Figure 3.12 : Mesh configuration of INSOLER with perforated air distributor.	105
Figure 3.13 : Grid independence test for objective 2.	106

Figure 3.14	: Comparison of predicted velocity across the perforation for different turbulence model with mathematical modelling.	107
Figure 3.15	: Selected plane for analysis (a) Planes parallel to yz-plane, (b) Planes parallel to xy-plane, (c) Planes parallel to xz-plane.	109
Figure 3.16	: Computational model of solar dryer with different chimney placement – (a) Case 1: External chimney, (b) Case 2: Interior chimney, (c) Case 3: Interior chimney with perforation.	111
Figure 3.17	: (a) Pictorial view of Integrated Solar Dryer (INSOLER). (b) Computational model of INSOLER (one compartment) with dimension.	112
Figure 3.18	: Mesh configuration of INSOLER with chimney.	113
Figure 3.19	: Comparison of predicted velocity at the chimney outlet for different turbulence model with mathematical modelling.	115
Figure 3.20	: Experimental and theoretical (CFD) collector outlet temperature for multiple-pass solar heat collector.	118
Figure 3.21	: Energy balance in Integrated Solar Dryer.	121
Figure 4.1	: Predicted fluid temperature across the middle region ($y=0.05\text{m}$) of solar heat collectors along the length of air passage.	127
Figure 4.2	: Temperature distribution of fluid at the middle region ($y = 0.05\text{ m}$) of air passage in (a) L-SHC and (b) T-SHC.	129
Figure 4.3	: Predicted local heat transfer coefficient (h_x) across the middle region ($y=0.05\text{m}$) of solar heat collectors along the length of air passage.	131
Figure 4.4	: Velocity vector of fluid across the middle region ($y=0.05\text{m}$) of air passage in (a) L-SHC and (b) T-SHC.	132
Figure 4.5	: Temperature distribution across the absorber in (a) L-SHC and (b) T-SHC, along with the corresponding temperature streamline in the air passage	133
Figure 4.6	: Pressure drop across the middle region ($y=0.05\text{m}$) of air passage in (a) L-SHC and (b) T-SHC.	134
Figure 4.7	: Variation of collector outlet temperature with mass flow rate for scale-up L-SHC.	136

Figure 4.8	: Variation of predicted collector efficiency (η_c) with mass flow rate for scale-up L-SHC.	136
Figure 4.9	: Variation of friction factor with mass flow rate for scale-up L-SHC.	138
Figure 4.10	: Variation of thermo-hydraulic performance factor with mass flow rate for scale-up L-SHC.	138
Figure 4.11	: Comparison of the predicted pressure drop across the perforation obtained through computational model and mathematical correlation.	140
Figure 4.12	: Turbulence kinetic energy distribution for case 1 at: (a) Plane PD, (b) Plane PE, (c) Plane PF, (d), Plane PH, (e) Plane PI, (f) Plane PJ.	143
Figure 4.13	: Turbulence kinetic energy distribution for case 2 at: (a) Plane PD, (b) Plane PE, (c) Plane PF, (d), Plane PH, (e) Plane PI, (f) Plane PJ.	144
Figure 4.14	: Turbulence kinetic energy distribution for case 3 at: (a) Plane PD, (b) Plane PE, (c) Plane PF, (d), Plane PH, (e) Plane PI, (f) Plane PJ.	145
Figure 4.15	: Temperature distribution for case 2 at: (a) Plane PA, (b) Plane PB, (c) Plane PC, (d) Plane PD, (e) Plane PE, and (f) Plane PF.	147
Figure 4.16	: Temperature distribution for case 3 at: (a) Plane PA, (b) Plane PB, (c) Plane PC, (d) Plane PD, (e) Plane PE, and (f) Plane PF.	148
Figure 4.17	: Positions of temperature measurement for uniformity analysis in objective 2.	149
Figure 4.18	: Temperature profile across the drying tray of case 2.	152
Figure 4.19	: Temperature profile across the drying tray of case 3.	152
Figure 4.20	: Comparison of the predicted velocity across the chimney obtained through computational model and mathematical correlation.	155
Figure 4.21	: Velocity distribution for case 1 at: (a) Plane PA, (b) Plane PB, (c) Plane PC, (d) Plane PD, (e) Plane PE, and (f) Plane PF.	158

Figure 4.22	: Velocity distribution for case 2 at: (a) Plane PA, (b) Plane PB, (c) Plane PC, (d) Plane PD, (e) Plane PE, and (f) Plane PF.	159
Figure 4.23	: Velocity distribution for case 1 at: (a) Plane PA, (b) Plane PB, (c) Plane PC, (d) Plane PD, (e) Plane PE, and (f) Plane PF.	160
Figure 4.24	: Temperature distribution for case 1 at: (a) Plane PA, (b) Plane PB, (c) Plane PC, (d) Plane PD, (e) Plane PE, and (f) Plane PF.	162
Figure 4.25	: Temperature distribution for case 2 at: (a) Plane PA, (b) Plane PB, (c) Plane PC, (d) Plane PD, (e) Plane PE, and (f) Plane PF.	163
Figure 4.26	: Temperature distribution for case 3 at: (a) Plane PA, (b) Plane PB, (c) Plane PC, (d) Plane PD, (e) Plane PE, and (f) Plane PF.	164
Figure 4.27	: Temperature profile across the drying tray of case 1.	167
Figure 4.28	: Temperature profile across the drying tray of case 2.	167
Figure 4.29	: Temperature profile across the drying tray of case 3.	168
Figure 4.30	: Computational model of INSOLER with different chimney placement studied – (a) Case 1: Interior chimney with perforation, (b) Case 2: Interior chimney, (c) Case 3: External chimney.	169
Figure 4.31	: Comparison of predicted velocity at the chimney outlet for different turbulence model with mathematical modelling.	171
Figure 4.32	: Pictorial view of Integrated Solar Dryer (INSOLER) – (a) Solidworks engineering drawing, (b) Prototype in Universiti Malaysia Sabah.	173
Figure 4.33	: Location of temperature measurement for INSOLER. experimental validation: (a) On the plane of computational model, (b) In the prototype	173
Figure 4.34	: Plot of experimental and CFD simulated drying air temperature vs time.	175
Figure 4.35	: Velocity distribution for case 1 at: (a) Plane PA, (b) Plane PB, (c) Plane PC, (d) Plane PD, (e) Plane PE, and (f) Plane PF.	177
Figure 4.36	: Velocity distribution for case 2 at: (a) Plane PA, (b) Plane PB, (c) Plane PC, (d) Plane PD, (e) Plane PE, and (f) Plane PF.	178
Figure 4.37	: Velocity distribution for case 3 at: (a) Plane PA, (b) Plane PB, (c) Plane PC, (d) Plane PD, (e) Plane PE, and (f) Plane PF.	179

Figure 4.38	: Velocity vector in the middle region for (a) Case 1, (b) Case 2, (c) Case 3.	180
Figure 4.39	: Temperature distribution for case 1 at: (a) Plane PA, (b) Plane PB, (c) Plane PC, (d) Plane PD, (e) Plane PE, and (f) Plane PF.	182
Figure 4.40	: Temperature distribution for case 2 at: (a) Plane PA, (b) Plane PB, (c) Plane PC, (d) Plane PD, (e) Plane PE, and (f) Plane PF.	183
Figure 4.41	: Temperature distribution for case 3 at: (a) Plane PA, (b) Plane PB, (c) Plane PC, (d) Plane PD, (e) Plane PE, and (f) Plane PF.	184
Figure 4.42	: Temperature profile across the drying tray of case 1.	187
Figure 4.43	: Temperature profile across the drying tray of case 2.	187
Figure 4.44	: Temperature profile across the drying tray of case 3.	188
Figure 4.45	: Positions of temperature and velocity measurement.	189
Figure 4.46	: Effect of mass flow rate on temperature profile along the height (H1 and H2) across the drying house.	190
Figure 4.47	: Effect of mass flow rate on temperature profile along the length (L) across the drying house.	191
Figure 4.48	: Effect of solar irradiance on temperature profile along the length (L1) across the drying house.	192

LIST OF NOMENCLATURES

A_c	-	Solar heat collector	m^2
$A_{ch,in}$	-	Cross-sectional area at chimney inlet	m^2
$A_{ch,out}$	-	Cross-sectional area at chimney outlet	m^2
A_{ch}	-	Cross-sectional area of chimney	m^2
A_{fl}	-	Surface area of drying house floor	m^2
A_p	-	Cross-sectional of pipe	m^2
A_r	-	Ratio of cross-sectional area of outlet over inlet	-
C_o	-	Discharge coefficient	-
Cp_d	-	Specific heat capacity of air @ T_d	$\text{kJ/kg } ^\circ\text{C}$
Cp_p	-	Specific heat capacity of product	$\text{kJ/kg } ^\circ\text{C}$
Cp_w	-	Specific heat capacity of water	$\text{kJ/kg } ^\circ\text{C}$
D_{hole}	-	Perforation diameter	mm
D_{pipe}	-	Pipe diameter	m
f_o	-	Friction factor without perforated air distributor	-
f_s	-	Friction factor of smooth heat collector	-
H_a	-	Ambient relative humidity	$\%$
h_f	-	Final enthalpy of drying	kJ/kg dry air
h_{fg}	-	Latent heat capacity @ T_d	kJ/kg K
H_{house}	-	Drying house height	m
h_i	-	Initial enthalpy of drying	kJ/kg dry air
k_t	-	Non-uniform coefficient	-
L_{house}	-	Drying house length	m
L_p	-	Pipe length	m
$m_{a,ch}$	-	Mass flow rate of air required at each chimney	m^3/s
$m_{a,pipe}$	-	Air flow rate in each inlet	kg/s
m_a	-	Mass flow of drying air required	kg/h
m_a	-	Total quantity of air required	kg/s
m_a	-	Mass flow rate of air required to remove moisture	m^3/s

M_p	-	Loading capacity per batch	kg
M_r	-	Moisture to be removed	kg
MC_f	-	Final moisture content	%
MC_i	-	Initial moisture content	%
n_c	-	Number of chimney	-
n_p	-	Number of air inlet	-
Nu_o	-	Nusselt number without perforated air distributor	-
Nu_s	-	Nusselt number of smooth heat collector	-
$Q_{loss,o}$	-	Heat loss through drying house outlet	W
$Q_{loss,SHC}$	-	Heat loss in solar heat collector	W
Q_r	-	Energy gained in drying house	W
Q_u	-	Energy gained in solar heat collector	W
T_a	-	Ambient air temperature	°C
T_d	-	Drying temperature	°C
T_{fl}	-	Temperature of floor surface	K
T_{rm}	-	Temperature of air in drying house	K
\bar{t}	-	Arithmetic average of temperature measured in each point.	K
t_s	-	Sunshine hour	hours
V_{ch}	-	Velocity produced in chimney	m/s
V_{in}	-	Wind speed	m/s
V_{pipe}	-	Air velocity in each pipe	m/s
W_f	-	Humidity ratio of humid air	kg water/kg of dry air
W_{house}	-	Drying house width	m
W_i	-	Humidity ratio of pure heated air	kg water/kg of dry air
η_c	-	Collector efficiency	%
$\rho_{air,c}$	-	Density of air in chimney	kg/m ³
ρ_d	-	Density of air @ T_d	kg/m ³
ρ_d	-	Density of air @ T_d	kg/m ³